

Effect of Local Structure Distortion on Superconductivity in Mg- and F-Codoped LaOBiS₂Haijie Chen,^{†,‡} Ganghua Zhang,[†] Tao Hu,[§] Gang Mu,[§] Wei Li,[§] Fuqiang Huang,^{*,†,‡} Xiaoming Xie,[§] and Mianheng Jiang[§][†]CAS Key Laboratory of Materials for Energy Conversion, Shanghai Institute of Ceramics, Chinese Academy of Sciences, Shanghai 200050, People's Republic of China[‡]State Key Laboratory of Rare Earth Materials Chemistry and Applications, College of Chemistry and Molecular Engineering, Peking University, Beijing 100871, People's Republic of China[§]State Key Laboratory of Functional Materials for Informatics, Shanghai Institute of Microsystem and Information Technology, Chinese Academy of Sciences, Shanghai 200050, People's Republic of China

Supporting Information

ABSTRACT: La_{1-x}Mg_xO_{1-2x}F_{2x}BiS₂ ($x = 0.1-0.35$) were synthesized, and their superconductive properties were investigated. The superconducting transition temperature (T_c) increased below the codoping level ($x \leq 0.25$). La_{1-x}Mg_xO_{0.6}F_{0.4}BiS₂ ($x = 0-0.2$) and La_{1-x}Mg_xO_{0.6}F_{0.4}BiS₂ ($x = 0.1-0.3$) were further prepared to explore the effect of Mg²⁺. We found that the introduction of Mg²⁺ and F⁻ leads to local structure distortion. Larger distortion is beneficial for superconductivity in LaOBiS₂, which was further confirmed by the results in La_{1-x}Ca_xO_{1-2x}F_{2x}BiS₂ ($x = 0.2, 0.3$).

The BiS₂-based superconductors have motivated considerable attention since the discovery of superconductivity ($T_c^{\text{onset}} = 8.6$ K) in Bi₄O₄S₃, which is constructed by superconducting [BiS₂]⁻ layers and blocking [Bi₄O₄(SO₄)_{1-δ}]⁺ layers.¹ Recently, new BiS₂-based superconducting compounds were found in doped LnOBiS₂ (Ln = La, Ce, Pr, Nd).²⁻⁹ These compounds possess layered structures and doping mechanisms similar to Fe- and Cu-based superconductors.¹⁰⁻¹³ The [BiS₂]⁻ layer plays a role similar to those of the [FePn]⁻ (Pn = P, As) layer in Fe-based superconductors and the [CuO₂]²⁻ layer in Cu-based ones. For better superconductivity, it is necessary to preserve the integrity of the conducting constituents, which have been demonstrated in both the Fe- and Cu-based superconductors. Herein, it can be expected that the superconductivity may be improved by modifying the [LnO]⁺ layers in the BiS₂-based superconductors, such as F⁻ doping in the O site² and trivalent ion doping in the Ln site.⁷

In Fe-based superconductors, doping in the [LnO]⁺ layers generates more carrier density and local structure distortion, as a result of the diverse valences and radii between the different ions.¹⁴ It has also been demonstrated that higher carrier (electron) density is beneficial for superconductivity in BiS₂-based superconductors.⁷ Furthermore, external high-pressure preparation methods have also been carried out to prepare the BiS₂-based superconductors, and a higher transition temperature (T_c) was also obtained.¹⁵⁻¹⁷ However, the effect of local structure distortion, which is different from that of the external

high pressure, needs to be explored. In our former research, we investigated the effect of lattice distortion on the superconductivity by codoping Mg²⁺/F⁻ and Sc³⁺/F⁻ into SmFeAsO.¹⁸⁻²⁰ Considering the similar layered structures between LaFeAsO and LaOBiS₂, Mg²⁺ and F⁻ were codoped into LaOBiS₂ and their superconductivity was fully investigated. Polycrystalline La_{1-x}Mg_xO_{1-2x}F_{2x}BiS₂ ($x = 0.1-0.35$) were synthesized. La_{1-x}Mg_xO_{0.6}F_{0.4}BiS₂ ($x = 0-0.2$), La_{1-x}Mg_xO_{0.6}F_{0.4}BiS₂ ($x = 0.1-0.3$), and La_{1-x}Ca_xO_{1-2x}F_{2x}BiS₂ ($x = 0.2, 0.3$) were prepared to understand the role of local structure distortion in LaOBiS₂.

The crystal structures of LaOBiS₂ and LaFeAsO are shown in Figure 1a. Both of them are crystallized in a layered structure with

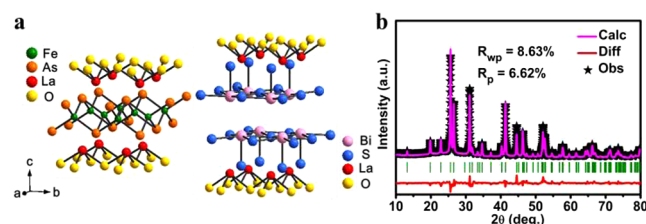


Figure 1. (a) Comparison of the crystal structures between LaOBiS₂ and LaFeAsO. (b) Fitted profiles of La_{0.8}Mg_{0.2}O_{0.6}F_{0.4}BiS₂ calculated by the Rietveld method.

alternate positive and negative layers. The structure of [BiS₂]⁻ layers (rock-salt-type) is different from that of [FeAs]⁻ layers (PbO-type). The [LaO]⁺ layer acts as a blocking layer in both compounds, and the [BiS₂]⁻ layer plays a role in LaOBiS₂ similar to that of the [FeAs]⁻ layer in LaFeAsO for charge transfer, which is crucial for superconductivity. In the Mg²⁺- and F⁻-codoped SmFeAsO, Mg²⁺ and F⁻ are preferred to substitute for Sm³⁺ and O²⁻, respectively.¹⁹ The same occupancies can be expected in LaOBiS₂. The Rietveld method was used to refine the crystal structure of La_{0.8}Mg_{0.2}O_{0.6}F_{0.4}BiS₂ with R_{wp} = 8.63% and R_p = 6.62%, and the fitted profile is shown in Figure 1b.

Received: August 28, 2013

Published: December 9, 2013

Substitution of O^{2-} by F^- leads to electron doping and La^{3+} by Mg^{2+} to hole doping. In the $La_{1-x}Mg_xO_{1-2x}F_{2x}BiS_2$ system, the introduction of Mg^{2+} generates x holes. Simultaneously, the introduction of F^- generates $2x$ electrons. The average oxidation state of Bi is $+(3-x)$ in $La_{1-x}Mg_xO_{1-2x}F_{2x}BiS_2$, and the electronic configuration of $Bi^{(3-x)+}$ becomes $Bi\ 6s^26p^x$. Herein, x electrons were introduced into n-type $LaOBiS_2$. A higher electron density was realized. First-principle density functional theory (DFT) calculations were performed by using the VASP code to obtain electronic density of states (DOS) for $LaOBiS_2$ and $La_{0.75}Mg_{0.25}O_{0.5}F_{0.5}BiS_2$ (Figure 2a). Compared to $LaOBiS_2$,

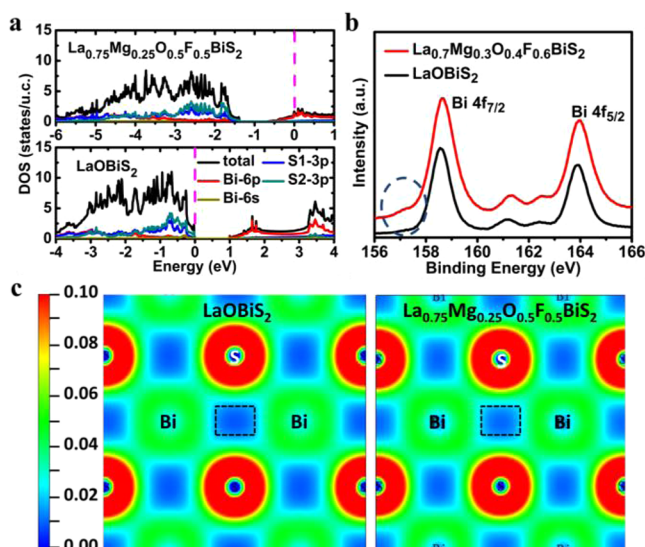


Figure 2. (a) Total and partial electronic DOS for $LaOBiS_2$ and $La_{0.75}Mg_{0.25}O_{0.5}F_{0.5}BiS_2$. (b) Bi 4f XPS spectra of the as-prepared $LaOBiS_2$ and $La_{0.7}Mg_{0.3}O_{0.4}F_{0.6}BiS_2$. (c) Charge density distribution ($0.1\ e/\text{\AA}^3$) on the Bi-S plane.

the Fermi level in $La_{0.75}Mg_{0.25}O_{0.5}F_{0.5}BiS_2$ moves upward toward the conduction band, resulting in a higher carrier density at the Fermi energy. Figure 2b shows Bi 4f X-ray photoelectron spectroscopy (XPS) spectra of the as-prepared $LaOBiS_2$ and $La_{0.7}Mg_{0.3}O_{0.4}F_{0.6}BiS_2$. The Bi 4f_{7/2} and Bi 4f_{5/2} XPS peaks centered at binding energies of 158.6 and 163.9 eV are typical for Bi-S bonds. In the marked area, the intensity of the curve in $La_{0.7}Mg_{0.3}O_{0.4}F_{0.6}BiS_2$ is stronger than that of $LaOBiS_2$, which indicates the existence of a smaller valence state of the Bi element. To further analyze the Bi-S bonds, the charge density distributions of $LaOBiS_2$ and $La_{0.75}Mg_{0.25}O_{0.5}F_{0.5}BiS_2$ are given in Figure 2c. The contour lines are plotted from 0.0 to $0.1\ e/\text{\AA}^3$. In the marked field, the area of the latter is smaller than that of the former, which indicates that the charge density near Bi atoms in $La_{0.75}Mg_{0.25}O_{0.5}F_{0.5}BiS_2$ is higher than that of $LaOBiS_2$. This result is consistent with DOS analysis and XPS spectra.

The X-ray diffraction (XRD) patterns of $La_{1-x}Mg_xO_{1-2x}F_{2x}BiS_2$ ($x = 0.1-0.35$) are shown in Figure 3a. An impurity of Bi_2S_3 is observed in the $x \geq 0.25$ samples, which is consistent with the former report.² The doping limit can be determined as $x = 0.25$. The main peaks are well indexed into space group $P4/nmm$ with a layered structure. The magnified XRD patterns between 25.0° and 27.5° are shown in Figure S3 in the Supporting Information (SI). The two peaks transfer right with increasing x until 0.25, indicating a shrunken lattice. The calculated lattice parameters (a and c) as a function of the doping level (x) are displayed in Figure S4 in the SI. The c parameter

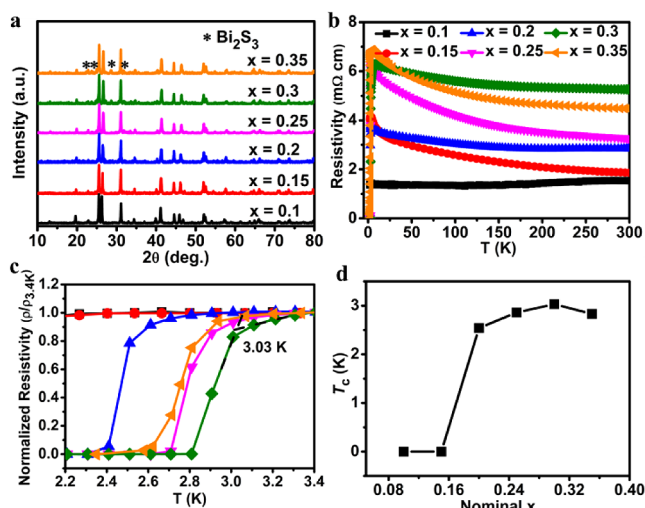


Figure 3. (a) Powder XRD patterns and (b) temperature dependence of bulk resistivity for $La_{1-x}Mg_xO_{1-2x}F_{2x}BiS_2$ ($x = 0.1-0.35$). (c) Magnified view near the transition temperature (T_c). (d) T_c as a function of the nominal doping (x).

decreases linearly with x below 0.25, which indicates that F^- and Mg^{2+} are successfully doped into the O and La sites, respectively. When $x \geq 0.25$, the parameters also become consistent.

Figure 3b shows the temperature dependence of resistivity for all of the samples. The resistivity increased with decreasing temperature, indicating semiconductor behavior before the superconductive transition. A magnification near the transition temperature (T_c) is presented in Figure 3c, where the resistivity is normalized. Clear superconducting resistivity transitions at low temperatures are observed with $x \geq 0.2$, as shown in Figure 3d. T_c increases with x below 0.3. As listed in Table S3 in the SI, no superconductivity is detected in $La_{0.9}Mg_{0.1}O_{0.8}F_{0.2}BiS_2$. T_c of $La_{0.7}Mg_{0.3}O_{0.4}F_{0.6}BiS_2$ (3.03 K) is higher than that of $La_{0.8}Mg_{0.2}O_{0.6}F_{0.4}BiS_2$ (2.54 K). Further doping generates smaller T_c . F^- doping can induce superconductivity in both Fe- and BiS_2 -based superconductors, and more F^- in the O site leads to higher T_c .^{2,10} Herein, as for $La_{1-x}Mg_xO_{1-2x}F_{2x}BiS_2$ ($x = 0.1-0.35$), the increase of T_c perhaps can be due to increased F^- doping. The effect of the introduction of Mg^{2+} is still uncertain.

To further evaluate the effect of partial replacement of Mg^{2+} for La^{3+} , $La_{1-x}Mg_xO_{0.6}F_{0.4}BiS_2$ ($x = 0-0.3$) were prepared at a fixed F^- doping level (0.4). The temperature dependence of resistivity near T_c and T_c as a function of the nominal doping (x) is shown in parts a and b of Figure 4, respectively. The introduction of Mg^{2+} suppresses T_c . As listed in Table S3 in the SI, compared to $LaO_{0.6}F_{0.4}BiS_2$ ($T_c = 2.98$ K), T_c (2.54 K) of $La_{0.8}Mg_{0.2}O_{0.6}F_{0.4}BiS_2$ is smaller. Substitution of divalent Mg^{2+} for trivalent La^{3+} introduces holes into the BiS_2 conduction layers, generating decreased carrier density in the n-type $LaOBiS_2$ system. Smaller Mg^{2+} (89 pm) replacing La^{3+} (116 pm) reduces lattice parameters, and results in local structure distortion.

In order to further explore the effect of local structure distortion, $La_{1-x}Ca_xO_{1-2x}F_{2x}BiS_2$ ($x = 0.2, 0.3$), in which divalent Ca^{2+} was introduced into the La^{3+} site, were prepared for further comparison, and the temperature dependence of resistivity is shown in Figure 4c. T_c of $La_{0.8}Ca_{0.2}O_{0.6}F_{0.4}BiS_2$ (2.07 K) is smaller than that of $La_{0.8}Mg_{0.2}O_{0.6}F_{0.4}BiS_2$ (2.54 K). Cell shrinkage of the former is smaller than that of the latter because of the smaller size difference between Ca^{2+} (112 pm) and La^{3+}

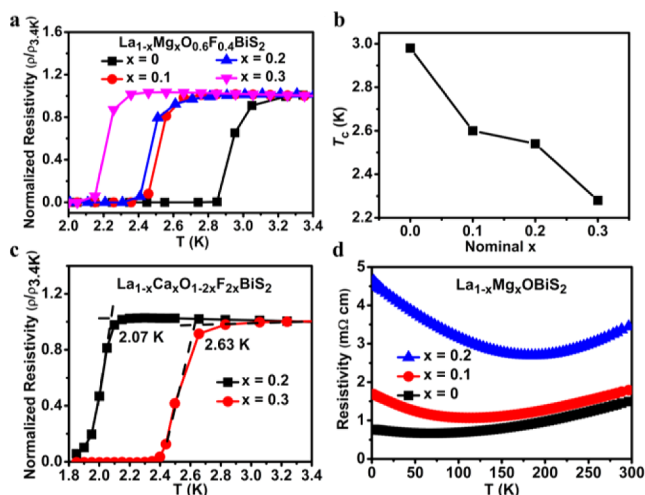


Figure 4. (a) Temperature dependence of bulk resistivity for La_{1-x}Mg_xO_{0.6}F_{0.4}BiS₂ ($x = 0-0.3$) near the transition temperature (T_c). (b) T_c as a function of the nominal doping (x). Temperature dependence of bulk resistivity for (c) La_{1-x}Ca_xO_{1-2x}F_{2x}BiS₂ ($x = 0.2, 0.3$) near the transition temperature (T_c) and (d) La_{1-x}Mg_xOBiS₂ ($x = 0-0.2$).

(116 pm), compared to that between Mg²⁺ (89 pm) and La³⁺ (116 pm). This demonstrates that larger local structure distortion is beneficial for superconductivity in LaOBiS₂, which can be further confirmed by a comparison of T_c between La_{0.7}Ca_{0.3}O_{0.4}F_{0.6}BiS₂ (2.63 K) and La_{0.7}Mg_{0.3}O_{0.4}F_{0.6}BiS₂ (3.03 K). In the Mg²⁺- and F⁻-codoped SmFeAsO system, the introduction of Mg²⁺ to the Sm site also brought in smaller electron density, but T_c was improved, which can be attributed to the results of local structure distortion.¹⁹ This was further confirmed in the latter Sc³⁺- and F⁻-codoped SmFeAsO system.²⁰ In the LaOBiS₂ system, lower T_c was obtained. This demonstrates that the superconductivity in LaOBiS₂ is less sensitive to structure distortion, compared to the carrier density. This is opposite to the result in the SmFeAsO system, in which structure distortion has a stronger impact.

As shown in Figure 4d, there is no superconductivity in the La_{1-x}Mg_xOBiS₂ ($x = 0-0.2$) samples, which is accordance with the results of Sr²⁺-doped LaOBiS₂.⁷ Hole doping cannot introduce superconductivity in BiS₂-based superconductors. The resistivity decreased initially with temperature, reached a minimum value, and then increased with temperature. The minimum value shifts to higher temperature at the higher doping level of Mg²⁺.

Mg²⁺ and F⁻ were codoped into LaOBiS₂ to explore the relationship between local structure distortion and superconductivity. Larger local structure distortion is beneficial for superconductivity in LaOBiS₂. Furthermore, the superconductivity in LaOBiS₂ is less sensitive to local structure distortion than carrier density, which is different in Fe-based superconductors.

■ ASSOCIATED CONTENT

Supporting Information

Experimental details, atomic positions and occupancies, microstructure, EDS spectra, magnified XRD patterns, lattice parameters, structure, upper critical field, and magnetic properties. This material is available free of charge via the Internet at <http://pubs.acs.org>.

■ AUTHOR INFORMATION

Corresponding Author

*E-mail: huangfq@mail.sic.ac.cn.

Notes

The authors declare no competing financial interest.

■ ACKNOWLEDGMENTS

This work was financially supported by Innovation Program of the CAS (Grant KJCX2-EW-W11), "Strategic Priority Research Program (B)" of the Chinese Academy of Sciences (Grants XDB04040200 and XDB04010600), NSF of China (Grants 91122034, 51125006, 51202279, 61376056, and 21201012), and Science and Technology Commission of Shanghai (Grant 12XD1406800).

■ REFERENCES

- (1) Singh, S. K.; Kumar, A.; Gahtori, B.; Sharma, G.; Patnaik, S.; Awana, V. P. S. *J. Am. Chem. Soc.* **2012**, *134*, 16504–16507.
- (2) Mizuguchi, Y.; Demura, S.; Deguchi, K.; Takano, Y.; Fujihisa, H.; Gotoh, Y.; Izawa, H.; Miura, O. *J. Phys. Soc. Jpn.* **2012**, *81*, 114725.
- (3) Li, B.; Xing, Z. W.; Huang, G. Q. *Europhys. Lett.* **2013**, *101*, 47002.
- (4) Jha, R.; Kumar, A.; Singh, S. K.; Awana, V. P. S. *J. Supercond. Novel Magn.* **2013**, *26*, 499–502.
- (5) Lin, X.; Ni, X. X.; Chen, B.; Xu, X. F.; Yang, X. X.; Dai, J. H.; Li, Y. K.; Yang, X. J.; Luo, Y. K.; Tao, Q.; Cao, G. H.; Xu, Z. *Phys. Rev. B* **2013**, *87*, 020504.
- (6) Xing, J.; Li, S.; Ding, X. X.; Yang, H.; Wen, H. H. *Phys. Rev. B* **2012**, *86*, 214518.
- (7) Yazici, D.; Huang, K.; White, B. D.; Jeon, I.; Burnett, V. W.; Friedman, A. J.; Lum, I. K.; Nallaiyan, M.; Spagna, S.; Maple, M. B. *Phys. Rev. B* **2013**, *87*, 174512.
- (8) Demura, S.; Mizuguchi, Y.; Deguchi, K.; Okazaki, H.; Hara, H.; Watanabe, T.; Denholme, S. J.; Fujioka, M.; Ozaki, T.; Fujihisa, H.; Gotoh, Y.; Miura, O.; Yamaguchi, T.; Takeya, H.; Takano, Y. BiS₂-based superconductivity in F-substituted NdOBiS₂. <http://arxiv.org/abs/1207.5248>.
- (9) Jha, R.; Kumar, A.; Singh, S. K.; Awana, V. P. S. Synthesis and superconductivity of new BiS₂ based superconductor PrO_{0.5}F_{0.5}BiS₂. <http://arxiv.org/abs/1208.5873>.
- (10) Kamihara, Y.; Watanabe, T.; Hirano, M.; Hosono, H. *J. Am. Chem. Soc.* **2008**, *130*, 3296–3297.
- (11) Chen, X. H.; Wu, T.; Wu, G.; Liu, R. H.; Chen, H.; Fang, D. F. *Nature* **2008**, *453*, 761–762.
- (12) Bednorz, J. G.; Müller, K. A. *Z. Phys. B: Condens. Matter* **1986**, *64*, 189–193.
- (13) Wu, M. K.; Ashburn, J. R.; Torng, C. J.; Hor, P. H.; Meng, R. L.; Gao, L.; Huang, Z. J.; Wang, Y. Q.; Chu, C. W. *Phys. Rev. Lett.* **1987**, *58*, 908–910.
- (14) Yang, J.; Ren, Z. A.; Che, G. C.; Lu, W.; Shen, X. L.; Li, Z. C.; Yi, W.; Dong, X. L.; Sun, L. L.; Zhou, F.; Zhao, Z. X. *Supercond. Sci. Technol.* **2009**, *22*, 025004.
- (15) Wolowiec, C. T.; Yazici, D.; White, B. D.; Huang, K.; Maple, M. B. *Phys. Rev. B* **2013**, *88*, 064503.
- (16) Selvan, G. K.; Kanagaraj, M.; Jha, R.; Awana, V. P. S.; Arumugam, S. Hydrostatic pressure dependence of superconductivity in PrO_{0.5}F_{0.5}BiS₂ superconductor. <http://arxiv.org/abs/1307.4877>.
- (17) Selvan, G. K.; Kanagaraj, M.; Esakki Muthu, S.; Jha, R.; Awana, V. P. S.; Arumugam, S. *Phys. Status Solidi R* **2013**, *7*, 510–513.
- (18) Fang, A. H.; Huang, F. Q.; Xie, X. M.; Jiang, M. H. *J. Am. Chem. Soc.* **2010**, *132*, 3260–3261.
- (19) Shi, S. L.; Fang, A. H.; Xie, X. M.; Huang, F. Q.; Jiang, M. H. *Chem. Mater.* **2011**, *23*, 3039–3044.
- (20) Chen, H. J.; Zheng, M.; Fang, A. H.; Yang, J. H.; Huang, F. Q.; Xie, X. M.; Jiang, M. H. *J. Solid State Chem.* **2012**, *194*, 59–64.